The Journal of Clinical Pharmacology
2022, 62(4) 555–567

DOI: 10.1002/jcph.1990

Population Pharmacokinetics of Ponatinib in Healthy Adult Volunteers and Patients With Hematologic Malignancies and Model-Informed Dose Selection for Pediatric Development

Michael J. Hanley, PharmD, PhD[1], Paul M. Diderichsen, PhD[2], Narayana Narasimhan, PhD[1,3], Shouryadeep Srivastava, MBBS, PhD[1,4], Neeraj Gupta, PhD[1], and Karthik Venkatakrishnan, PhD[1,5]

Abstract

The *BCR-ABL1* inhibitor ponatinib is approved for the treatment of adults with chronic myeloid leukemia or Philadelphia chromosome–positive acute lymphoblastic leukemia, including those with the T315I mutation. We report a population pharmacokinetic model-based analysis for ponatinib and its application to inform dose selection for pediatric development. Plasma concentration–time data were collected from 260 participants (86 healthy volunteers; 174 patients with hematologic malignancies) enrolled across 7 clinical trials. Data were analyzed using nonlinear mixed-effects modeling. Ponatinib pharmacokinetics were described by a 2-compartment model with first-order elimination from the central compartment. The final model included body weight and age as covariates on the apparent central volume of distribution; however, exposure variability explained by these covariates was small compared with overall variability in the population. None of the covariates evaluated, including sex, age (19-85 years), race, body weight (40.7-152.0 kg), total bilirubin (0.1-3.16 mg/dL), alanine aminotransferase (6-188 U/L), albumin (23.0-52.5 g/L), and creatinine clearance (≥28 mL/min) had clinically meaningful effects on apparent oral clearance. Simulations based on the final model predicted that daily doses of 15 to 45 mg result in steady-state average concentrations that are in the pharmacological range for *BCR-ABL1* inhibition and approximate or exceed concentrations associated with suppression of T315I mutant clones. The final model was adapted using allometric scaling to inform dose selection for pediatric development. Clinicaltrials.gov identifier: NCT00660920; NCT01667133; NCT01650805

Keywords

acute lymphoblastic leukemia, BCR-ABL, chronic myeloid leukemia, pediatric, pharmacokinetics, Philadelphia chromosome, ponatinib, tyrosine kinase inhibitors

Ponatinib is an oral, small-molecule, tyrosine kinase inhibitor (TKI) with activity against native and mutated *BCR-ABL1*, including the T315I mutant, which is resistant to all other TKIs approved for use in patients with chronic myeloid leukemia (CML) or Philadelphia chromosome–positive (Ph+) acute lymphoblastic leukemia (ALL).[1–3] In the United States, ponatinib is indicated for the treatment of adult patients with chronic-phase CML with resistance or intolerance to at least 2 prior kinase inhibitors; patients with accelerated-phase or blast-phase CML or Ph+ ALL for whom no other TKI therapy is indicated; and patients with the T315I mutation.[4] The pivotal phase 2 PACE (Ponatinib Ph+ ALL and CML Evaluation) trial in patients with CML or Ph+ ALL who were resistant or intolerant to dasatinib or nilotinib or had the T315I mutation demonstrated significant antileukemic activity of ponatinib at a starting dose of 45 mg once daily.[5,6] With a median follow-up of 56.8 months (range, 0.1-73.1 months) in heavily pretreated patients with chronic-phase CML, Kaplan-Meier estimates of 5-year progression-free survival and 5-year overall survival were 53% and 73%, respectively.[6]

[1]Millennium Pharmaceuticals, Inc., a wholly owned subsidiary of Takeda Pharmaceutical Company Limited, Cambridge, Massachusetts, USA
[2]Certara, Princeton, New Jersey, USA
[3]Current affiliation: Verastem Oncology, Needham, Massachusetts, USA
[4]Current affiliation: iTeos Therapeutics, Cambridge, Massachusetts, USA
[5]Current affiliation: EMD Serono, Inc., Billerica, Massachusetts, USA

Submitted for publication 20 July 2021; accepted 21 October 2021.

Corresponding Author:
Michael J. Hanley, PharmD, PhD, Millennium Pharmaceuticals, Inc., a wholly owned subsidiary of Takeda Pharmaceutical Company Limited, 40 Landsdowne Street, Cambridge, MA 02139, USA
Email: Michael.Hanley@takeda.com

Clinical studies have demonstrated that ponatinib is readily absorbed following oral administration, with peak concentrations observed within 6 hours after oral administration.[4,7–13] Ponatinib exhibits approximately dose-proportional increases in exposure (maximum concentration [C_{max}] and area under the concentration-time curve [AUC]) over the dose range of 2 to 60 mg.[4,13] Ponatinib is metabolized through multiple pathways, primarily by cytochrome P450 (CYP) 3A4 and to a lesser extent by CYP2C8, CYP2D6, and CYP3A5, as well as by esterases and/or amidases.[4,7] Drug-drug interaction studies showed that coadministration of ketoconazole (a strong CYP3A inhibitor) increased ponatinib C_{max} and AUC from time 0 to infinity ($AUC_{0-\infty}$) by 47% and 78%, respectively,[9] whereas coadministration of rifampin (a strong CYP3A inducer) reduced ponatinib C_{max} and $AUC_{0-\infty}$ by 42% and 62%, respectively.[4,11] Following administration of a single oral dose of radiolabeled ponatinib, ≈87% of the radioactive dose was recovered in the feces and ≈5% in the urine.[4,7]

The objectives of this analysis were to develop a population pharmacokinetics (PK) model based on available data from phase 1, 1/2, and 3 ponatinib studies in adult patients and healthy volunteers, including the identification and quantification of clinically relevant covariates on population PK parameters, and to estimate individual PK parameters for patients included in the analysis based on the final population PK model. Additionally, the final PK model was adapted for pediatric patients to support dose selection for pediatric development.

Methods

Data Collection

The protocols of all 7 studies included in this population PK analysis were approved by the appropriate local institutional review boards (IRBs) or independent ethics committees. Studies AP24534-11-102, AP24534-11-103, AP24534-12-107, and AP24534-12-108 were approved by Institutional Review Board Services Ontario.[8–11] The Japanese phase 1/2 study (AP24534-11-106, NCT01667133) was approved by IRBs or independent ethics committees of the 9 participating centers in Japan.[12] The phase 1 study (AP24534-07-101, NCT00660920) was approved by the IRB at each of the 5 study centers.[13] The phase 3 EPIC (Evaluation of Ponatinib Versus Imatinib in Chronic Myeloid Leukemia) study (AP24534-12-301, NCT01650805) was approved by the IRBs or independent ethics committees of the 106 study sites enrolling patients.[14] All participants provided written informed consent.

Ponatinib plasma concentration–time data were collected from adult healthy volunteers and patients with hematologic malignancies who had participated in 1 of 7 clinical trials.[8–14] Participant eligibility criteria for each study are described in the original publications. Table S1 provides a summary of the studies included in the population PK analysis. For the food-effect study in healthy volunteers,[8] only data collected under fasted conditions were included in the population PK analysis. For the drug-drug interaction studies in healthy volunteers,[9–11] ponatinib data collected in the presence of the coadministered drug (ie, ketoconazole, rifampin, or lansoprazole) were excluded from the population PK analysis. All study procedures were performed in accordance with the International Council for Harmonisation Good Clinical Practice guidelines and appropriate regulatory requirements.

Plasma concentrations of ponatinib were measured using 2 validated liquid chromatography–tandem mass spectrometry assays.[8–10,13]

Population PK Modeling

The population PK analysis was performed using NONMEM (version 7.3; ICON Development Solutions, Hanover, Maryland[15]) for nonlinear mixed-effects models, running under Perl-speaks-NONMEM (version 4.6) on a grid of CentOS 7.1 Linux servers and the Fortran compiler (version 12.0.4; Intel, Santa Clara, California). Analysis of results and simulations was performed using R (version 3.4.3; R Foundation for Statistical Computing, Vienna, Austria[16]).

For development of the base population PK model, fixed-effect model parameters (θ), variances of the interindividual variability (ω^2), and residual error (σ^2) were estimated. Interindividual variability was implemented by exponential random-effect models, corresponding to log-normally distributed individual parameters, and was defined as:

$$\theta_i = \theta_{\mathrm{TV,i}} \cdot \exp(\eta_i) \quad (1)$$

where θ_i and θ_{TV} are individual and typical values of the parameter (eg, apparent oral clearance [CL/F]). η_i is an individual-level random variable sampled from a normal distribution with a mean of 0 and variance of ω^2, and it represents the ith individual's deviation from the typical value. Initially, random effects were assumed to be independent; however, random-effect models defined by a nondiagonal variance-covariance matrix (Ω) were preferred if they resulted in meaningful improvements in model fit.

Models describing untransformed data, as well as data that were log-transformed on both sides, were evaluated during model development. In models applying the log-transformed on both sides approach, the residual unexplained variability was described by

an additive (on the log-scale) error model that was parameterized as:

$$\log(Y_{ik}) = \log(C_{ik}) + \varepsilon_{ik} \quad (2)$$

where Y_{ik} was the kth observed concentration in the ith individual, C_{ik} was the corresponding individual model-predicted concentration, and ε_{ik} was the residual error sampled from a normal distribution with a mean of 0 and variance of σ^2. Alternative residual error models with >1 ε were considered with a covariance matrix Σ to define the variances and covariances of the ε's. Initially, the ε's were assumed to be uncorrelated. Nondiagonal Σ was estimated to evaluate if the data supported estimation of correlations between ε's.

Appropriate transformations of parameters were considered to appropriately constrain parameter values. For example, log transformation of CL/F was considered to constrain the estimate to positive values. Similarly, logit transformations were considered for parameters describing the fraction of a dose to constrain the estimate to between 0 and 1.

Shrinkage of interindividual random effects (η) was evaluated for diagnostic purposes. The shrinkage for a structural parameter sh_θ (η shrinkage) was calculated as[17]:

$$sh_\theta = 1 - \frac{SD(\eta_{EBE,\theta})}{\omega_\theta} \quad (3)$$

where $SD(\eta_{EBE,\theta})$ is the standard deviation of the individual η for θ, and ω_θ is the model estimate of the SD associated with θ.

Covariate Model Development

Continuous covariates (age, body weight, albumin, alanine aminotransferase [ALT], total bilirubin, and creatinine clearance [CrCL]) and categorical covariates (race, patient or healthy volunteer status, and sex) were tested in the development of the covariate model (Table S2). Continuous covariates were included in the model as power functions, while binary covariates were implemented as factors:

$$\theta_{TV,i} = \theta_{TV,Pop} \cdot \left(\frac{x_{Cont,i}}{median(x_{Cont,i})}\right)^{\theta_1} \cdot (1 + x_{Cat,i} \cdot \theta_2) \quad (4)$$

In this equation, the parameter $\theta_{TV,i}$ for the ith subject is defined as a function of the population typical value, $\theta_{TV,Pop}$, and the individual contributions from continuous ($x_{Cont,i}$) and binary ($x_{Cat,i}$ with values 0 and 1) covariates. θ_1 and θ_2 represent the respective covariate coefficients.

A stepwise covariate modeling strategy (single addition, forward inclusion, and backward elimination) was performed.[18] Model selection was based on the likelihood ratio test. During the forward inclusion step, statistical significance of a covariate effect was evaluated using the chi-square test for $P < .01$. Covariates that were statistically significant were retained in the model. In the backward elimination phase, statistical significance of covariate effects was evaluated using the chi-square test for $P < .001$. Significant covariates were retained, and covariates whose removal did not lead to a significant worsening of the objective function value (OFV) were iteratively dropped until no such nonsignificant covariates ($P > .001$) remained in the model. Finally, covariate effects that were imprecisely estimated (% relative standard error [%RSE] >50%; that is, the 95% confidence interval included 0) were considered for exclusion from the covariate model.

Model Evaluation and Qualification

Nested models were compared using the likelihood ratio test. Structural and residual error model discrimination were based on standard model diagnostics, such as a decrease in the OFV, precision and accuracy of parameter estimation (%RSE), condition number, successful model convergence and covariance step, and examination of goodness-of-fit plots and prediction-corrected visual predictive checks (VPCs). In the VPCs, percentiles (median, 5th, and 95th percentiles) of observed data were superimposed on those of the individual model-predicted ponatinib concentration-time profiles, based on 250 simulated replicates of the analysis data set. Model robustness and parameter estimates were assessed by bootstrap based on 1000 resampled data sets with replacement up to the total number of patients in the original data set.

Simulations

The final population PK model was used to perform simulations for patients treated with daily ponatinib doses of 15, 30, and 45 mg. Individual plasma concentration–time profiles of ponatinib were simulated for the typical patient and 1000 virtual patients to describe ponatinib plasma concentrations with each once-daily dosing regimen, relative to reference concentrations of 10.7 ng/mL (20 nM) and 21.3 ng/mL (40 nM), which have been previously demonstrated to suppress most *BCR-ABL1* mutants and T315I *BCR-ABL1* mutants, respectively, in cell-based mutagenesis assays.[1] For the typical patient, random effects were set to zero, and covariate values were set to the median value in the analysis data set. For virtual patients, random effects were sampled from the random effects variance–covariate matrix and covariates were sampled from distributions designed to reflect values reported in the data set. The 5th and 95th percentiles of the concentration-time profiles were derived from

the profiles of the 1000 virtual patients. The AUC, C_{max}, trough concentration, and average concentration ($C_{average}$) were derived for each simulated patient and summarized.

Model-Informed Dose Selection for Pediatric Development

A primary objective of the pediatric program for ponatinib is to evaluate its safety and efficacy in combination with multiagent chemotherapy for the treatment of pediatric patients ≥1 year of age with Ph+ ALL. A 30-mg dose is being evaluated in combination with chemotherapy in adult patients with Ph+ ALL (ClinicalTrials.gov Identifier: NCT03589326). Accordingly, a model-informed approach was used to establish pediatric posology to approximately match adult exposures at 30 mg for the design of a pediatric study (ClinicalTrials.gov Identifier: NCT04501614).

For the purpose of predicting pediatric doses that would match adult exposures at ponatinib 30 mg once daily, the developed model was adapted by removing the previously estimated adult covariate effects and including allometric scaling coefficients of 0.75 and 1 for clearance and volume parameters, respectively. The adapted model, through simulation, was used to predict the target exposure (AUC) in adult patients and to simulate pediatric exposures after administration of fixed doses of ponatinib. Virtual pediatric patients were simulated on the basis of body size vs age distributions from the National Health and Nutrition Examination Survey data set provided by the Centers for Disease Control and Prevention.[19] A pediatric population consisting of 250,000 virtual pediatric patients was simulated on the basis of a stepwise uniform pediatric age distribution designed to mimic the age distribution published for an imatinib study in pediatric Ph+ ALL and stratified by sex (50:50 male to female).[20] The pediatric simulations assumed similar bioavailability between the age-appropriate formulation(s) and the currently available tablet formulation.

Results

Data Summary

The population PK analysis included data from 260 participants (86 healthy volunteers and 174 patients with hematologic malignancies; Table S1). The analysis population was predominantly male (68.8%) and White (71.5%) with a median age of 49 years (range, 19-85 years; Table S3). A total of 2637 PK samples were available, of which 121 (4.6%) were below the limit of quantification. Given the low number of samples below the limit of quantification, they were excluded from the analysis.

Population PK Model

The observed ponatinib PK data were described by a 2-compartment model with first-order elimination from the central compartment (Figure 1). Of note, a 3-compartment model did not result in a meaningful improvement in goodness-of-fit and was associated with imprecise estimates of the apparent volume of the second peripheral compartment (RSE >100%), thereby supporting the selection of a 2-compartment model. For healthy subjects, absorption of ponatinib into the central compartment was best described by two parallel processes where a fraction of the dose (F1) was absorbed via 2 sequential transit compartments and the remaining fraction (F2) was described by first-order absorption with a lag time. However, for patients, first-order absorption with a lag time was not required to describe the PK of ponatinib, which is likely explained by the richer serial PK sampling schedules during the absorption phase in healthy subject studies compared with the patient studies. Thus, the value of F2 was set to 0 for patients. The first-order rate constant describing the second absorption route (K_{a2}) for the F2 route was associated with considerable parameter uncertainty (RSE >100%) in preliminary model evaluation. Therefore, K_{a2} was fixed to a value of 4.41 based on its estimate in initial runs during base model development.

For the F1 route, an absorption model with the estimated number of transit compartments based on the Stirling approximation was initially evaluated.[21] The number of transit compartments estimated by this initial model was 0.5, suggesting that the model could be simplified by including a number of explicitly defined transit compartments. Models containing 1 and 2 transit compartments were therefore evaluated. Despite being closer to the estimated number of transit compartments, an alternative model with 1 transit compartment resulted in a worse description of the data than the model with 2 transit compartments. Consequently, a transit model consisting of 2 explicitly defined transit compartments was included to describe absorption via the F1 route in the base population PK model.

The base model included interindividual variability on the rate constant of absorption through the F1 route (K_{tr}, identical to the first-order absorption rate constant via the F1 route [K_{a1}]), CL/F, and the apparent central volume of distribution (V3/F). Additionally, a correlation between the random effects on CL/F and V3/F was introduced in the base model, which reduced the OFV by 42.48 points. The residual error model included distinct terms to characterize the unexplained variability in patients and healthy subjects reflecting the richer serial PK sampling schedule in the healthy volunteer studies.

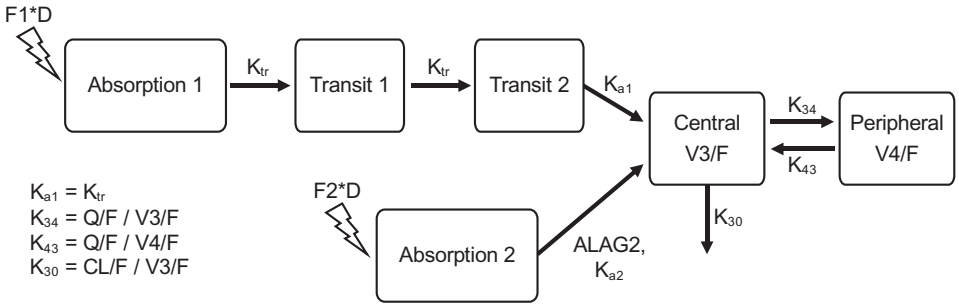

Figure 1. Structural model describing the pharmacokinetics of ponatinib. ALAG2, absorption lag time from the second absorption compartment; CL/F, apparent oral clearance; D, dose; F1, fraction of absorbed dose entering in the central compartment via the first absorption compartment; F2, fraction of absorbed dose entering in the central compartment via the second absorption compartment; K_{a1}, first-order absorption rate constant via the F1 route; K_{a2}, first-order absorption rate constant via the F2 route; K_{tr}, transit rate constants from the first absorption compartment to the central compartment (identical to K_{a1}); K_{34} and K_{43}, distributional rate constants between the central and peripheral compartments; K_{30}, elimination rate constant from the central compartment; Q/F, apparent distributional clearance; V3/F, apparent central volume of distribution; V4/F, apparent peripheral volume of distribution.

Table 1. Final Population PK Model Parameters

Parameter	Estimate	RSE (%)	Bootstrap 95%CI	Shrinkage (%)
K_{a2}	4.41/h	fixed	(4.41-4.41)	…
CL/F	34.28 L/h	3.23	(32.01-36.5)	…
V3/F	838.6 L	3.56	(778.8-899.1)	…
Q/F	17.21 L/h	7.33	(14.91-19.98)	…
V4/F	347.4 L	5.25	(311.8-385.6)	…
Absorption lag time (ALAG2)	3.932 h	0.271	(3.911-3.952)	…
K_{a1} (= K_{tr})	1.302/h	4.06	(1.199-1.407)	…
F2	46.61%	94.4[a]	(39.48-52.57)	…
Effect of age on V3/F	$(Age/49)^{0.6447}$	16.7	(0.4225-0.8653)	…
Effect of body weight on V3/F	$(Body\ weight/77.15)^{0.5038}$	30.4	(0.2053-0.8278)	…
Residual unexplained variability				
Healthy volunteers	14.91%[b]	5.01[c]	(13.39-16.34)	13%
Patients with hematologic malignancies	38.59%[b]	20.1[c]	(27.17-53.74)	10%
Interindividual variability				
K_{a1}	46.85%[b]	6.84[c]	(40.56-53.12)	19%
CL/F	48.04%[b]	6.03[c]	(42.28-54.29)	6.4%
V3/F	42.33%[b]	9.88[c]	(34.09-49.79)	20%
Correlation between CL/F and V3/F	63.68%	9.31[c]	(50.93-75.26)	…

ALAG2, absorption lag time from the second absorption compartment; CI, confidence interval; CL/F, apparent oral clearance; F2, fraction of absorbed dose entering in the central compartment via the second absorption compartment; K_{a1}, first-order absorption rate constant via the F1 route; K_{a2}, first-order absorption rate constant via the F2 route; K_{tr}, transit rate constants from the first absorption compartment to the central compartment (identical to K_{a1}); Q/F, apparent distributional clearance; RSE, relative standard error; V3/F, apparent central volume of distribution; V4/F, apparent peripheral volume of distribution.

[a] %RSE given on the logit scale.

[b] Residual and interindividual variability are shown as % coefficient of variation.

[c] %RSE given on the (co)variance scale.

Multivariate stepwise covariate modeling identified age and body weight as the 2 most statistically significant covariates on V3/F. In a third forward addition step, the effect of age on CL/F was included ($P = .007$); however, this parameter-covariate relationship was removed during backward elimination. Accordingly, the final model only included age and body weight as covariates on V3/F.

The PK parameter values estimated for the final population PK model are presented in Table 1. Final model parameters were estimated with good precision with RSE <31% with the exception of F2, which had an estimated RSE of 94%. The F2 parameter represented a fraction and was implemented as a logit-transformed parameter. Accordingly, a value of F2 = 0 for the transformed parameter corresponded to 50% absorption through each route of absorption. In addition, for patients, the entire absorbed dose entered the central compartment via the F1 route; therefore, the higher RSE on the F2 parameter was not considered to impact the characterization of ponatinib PK in patients. Shrinkage of random effects on CL/F,

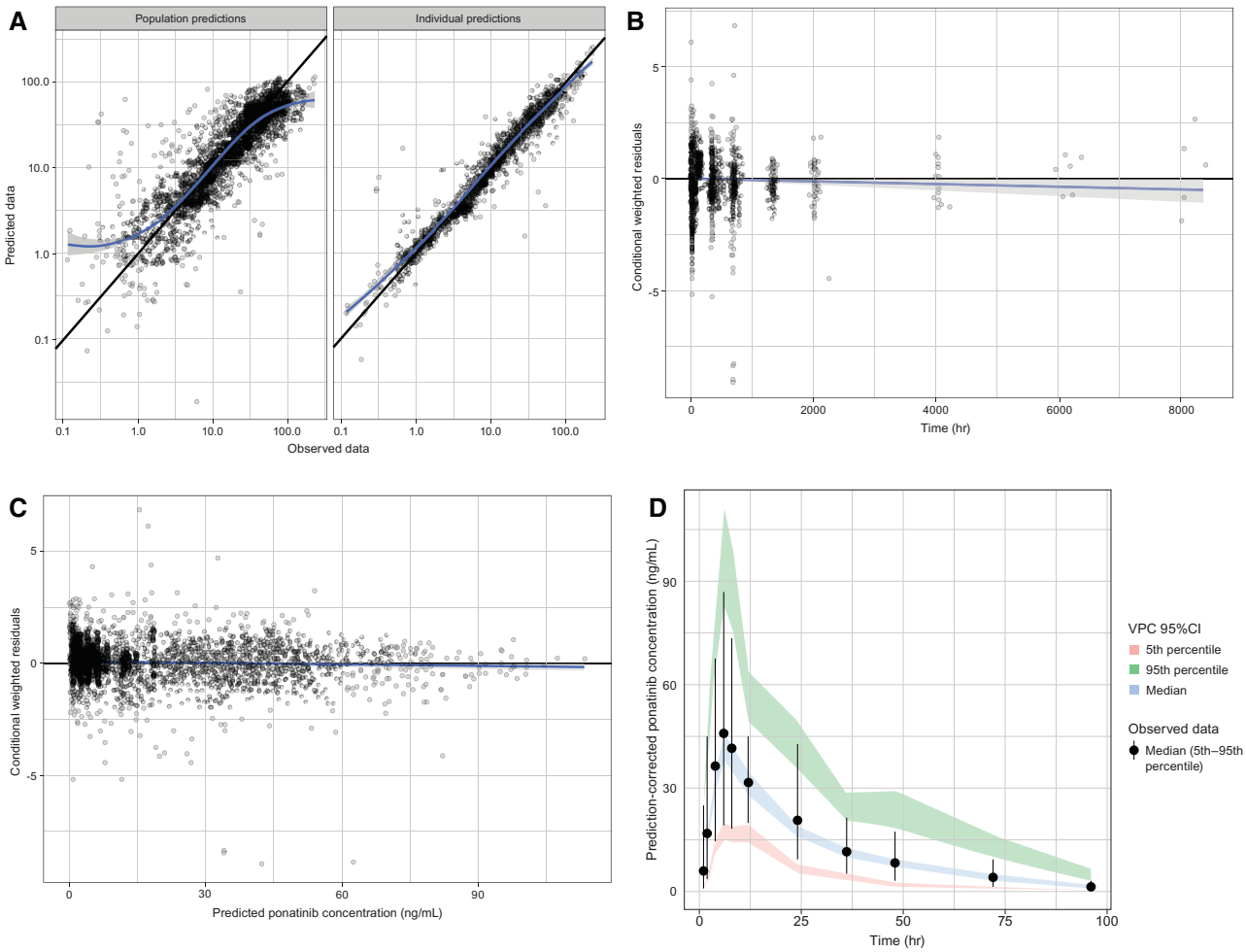

Figure 2. Diagnostic plots. (A) Goodness-of-fit plots of the final model based on population-predicted vs observed plasma ponatinib concentrations (left) and individual-predicted vs observed plasma ponatinib concentrations (right). Circles represent individual data, black solid lines represent the identity line, and blue solid lines are LOESS curves. The gray shaded areas represent the 95%CI of the LOESS curves. (B) Conditional weighted residuals vs time since first dose. (C) Conditional weighted residuals vs predicted plasma ponatinib concentration. In (B) and (C), circles represent individual data, and the blue solid line with a gray-shaded area shows a linear regression with 95%CI. (D) VPC of the final model for the overall analysis population. Black circles (whiskers) represent the median (90% range) of observed plasma ponatinib concentrations, and the colored shaded regions represent the 95%CIs of predicted 50th (blue), 5th (red), and 95th percentile (green) concentrations. CI, confidence interval; LOESS, locally estimated scatterplot smoothing; VPC, visual predictive check.

V3/F, and K_{a1} was <20%. Residual error was best described as log additive with distinct terms describing the unexplained variability for patients separately from healthy volunteers. The residual variability expressed as the coefficient of variation was ≈15% for healthy volunteers and 39% for patients. The condition number, a measure of collinearity between parameter estimates, was acceptable at 29.32.

Ponatinib CL/F was estimated at 34.28 L/h with an interindividual variability of 48.0%, indicating that 90% of the population would be expected to have a ponatinib CL/F between 15.55 and 75.54 L/h. The V3/F was estimated at 838.6 L with interindividual variability of 42.3%, indicating that 90% of the population with the same age and body weight would have a V3/F between 418 and 1682 L.

Goodness-of-fit plots demonstrated close agreement between the observed and individual predicted ponatinib concentrations (Figure 2A). Although some bias was observed at the population level for the lowest and highest concentrations, the majority of data points fell along the line of unity. Conditional weighted residuals over time plots supported that the residual error model was appropriately specified and independent of time (Figure 2B and C). In the bootstrap analysis of the final covariate model, all of the 1000 bootstrap replicates (100%) achieved successful convergence. Parameter estimates based on the analysis data set were in good agreement with the 95% confidence interval of parameter values based on the bootstrap analysis (Table 1). A prediction-corrected VPC of the final model confirmed that the model was appropriately

Table 2. Simulations of Steady-State Ponatinib Exposure Metrics for a Typical Patient and the Percentage of Patients Achieving $C_{average}$ Above Reference Concentrations Associated With *BCR-ABL1* Inhibition in Cell-Based Assays

	Daily Ponatinib Dose		
	15 mg	30 mg	45 mg
AUC_{SS}, μg · h/mL (90% PI)	0.438 (0.199-0.981)	0.875 (0.398-1.96)	1.31 (0.598-2.94)
$C_{averageSS}$, ng/mL (90% PI)	18.2 (8.3-40.9)	36.5 (16.6-81.7)	54.7 (24.9-123)
C_{maxSS}, ng/mL (90% PI)	24.6 (12.2-53)	49.3 (24.4-106)	73.9 (36.6-159)
$C_{troughSS}$, ng/mL (90% PI)	12.5 (4.06-31.4)	25 (8.12-62.9)	37.5 (12.2-94.3)
$C_{averageSS} > 10.7$ ng/mL,[a] % of patients	87.2	99.4	99.9
$C_{averageSS} > 21.3$ ng/mL,[b] % of patients	34.7	87.2	97.2

AUC_{SS}, area under the plasma concentration–time curve at steady state; $C_{averageSS}$, average concentration at steady state; C_{maxSS}, maximum concentration at steady state; $C_{troughSS}$, predose concentration at steady state; PI, prediction interval.

90% PI, 5th to 95th percentile prediction interval.

[a] Concentration associated with inhibition of *BCR-ABL1* in cell-based assays.

[b] Concentration associated with inhibition of *BCR-ABL1* T315I mutants in cell-based assays.

specified (Figure 2D). Stratification of the VPC by dose, study, and population (ie, patient vs healthy volunteers) indicated the absence of readily apparent sources of heterogeneity in ponatinib PK by these factors.

Based on the final model, the individual predicted steady-state AUC of ponatinib for a 45-mg dose, calculated as $AUC_i = 45$ mg/(CL/F_i), was evaluated vs relevant covariates using linear regression analyses. Figure 3 shows the correlations between individual predicted exposure and the continuous covariates of age (Figure 3A), body weight (Figure 3B), albumin (Figure 3C), total bilirubin (Figure 3D), CrCL (Figure 3E), and ALT values (Figure 3F). Across the entire analysis population, the 5th and 95th percentiles of individual predicted exposures were −51.8% and +113% relative to the median AUC, respectively. The AUC at the 5th and 95th percentiles of continuous covariates relative to the AUC at the median covariate value was at most 14.5% for any covariate, which was well below the variability in individual predicted AUC across the entire analysis population. Similarly, for categorical covariates of sex (Figure 3G), population (ie, healthy volunteer or patient; Figure 3H) and race (Figure 3I), the magnitude of relative difference in predicted AUC for each category was at most 15.1% compared to the most common category, which was below the total variability in individual predicted AUC across the entire analysis population. Additionally, these differences are substantially lower than the reported overall variability for ponatinib PK (coefficient of variation of 73% for AUC).[4] Figure 4 illustrates the magnitude of covariate effects relative to the overall population of ponatinib exposures. Taken together, these analyses confirmed the absence of clinically meaningful effects of the covariates of interest on the systemic exposure (AUC) of ponatinib and were consistent with these covariates not having clinically meaningful effects on CL/F.

Model-Based Simulations

Simulated ponatinib concentration-time profiles for the typical patient and the 5th to 95th percentile ranges across 1000 virtual patients following once-daily administration of 15, 30, or 45 mg ponatinib over the first week of treatment and on day 28 are shown in Figure 5. Steady-state ponatinib PK parameters for a typical patient and the associated 90% prediction interval for the simulated population are summarized in Table 2. Based on the model simulations, the AUC and $C_{average}$ at steady state following treatment with 45 mg of ponatinib once daily in the typical patient (90% prediction interval) were 1.31 μg·h/mL (0.598-2.94) and 54.7 ng/mL (24.9-123), respectively. For 30 mg once daily and 15 mg once daily, the corresponding values for AUC were 0.875 μg·h/mL (0.398-1.96) and 0.438 μg·h/mL (0.199-0.981), respectively, and for $C_{average}$ were 36.5 ng/mL (16.6-81.7) and 18.2 ng/mL (8.3-40.9), respectively. Over the 15- to 45-mg dose range, there was an increase in the percentage of simulated patients achieving $C_{average}$ values associated with inhibition of *BCR-ABL1* (>10.7 ng/mL) and T315I mutants (>21.3 ng/mL) in cell-based assays.

Allometric Scaling of the Population PK Model for Pediatric Dose Selection

The developed population PK model was subsequently adapted using allometric scaling to inform pediatric dose selection. Simulations were performed to identify pediatric doses that would result in systemic exposures comparable to those observed at an adult reference dose of 30 mg. Results of the pediatric simulations (Figure 6) indicated that ponatinib doses of 5 mg, 10 mg, 20 mg, or 30 mg for patients weighing ≥5 and <15 kg, ≥15 and <30 kg, ≥30 and <45 kg, and ≥45 kg are anticipated to result in systemic exposures that approximately match adult exposures following a 30-mg dose.

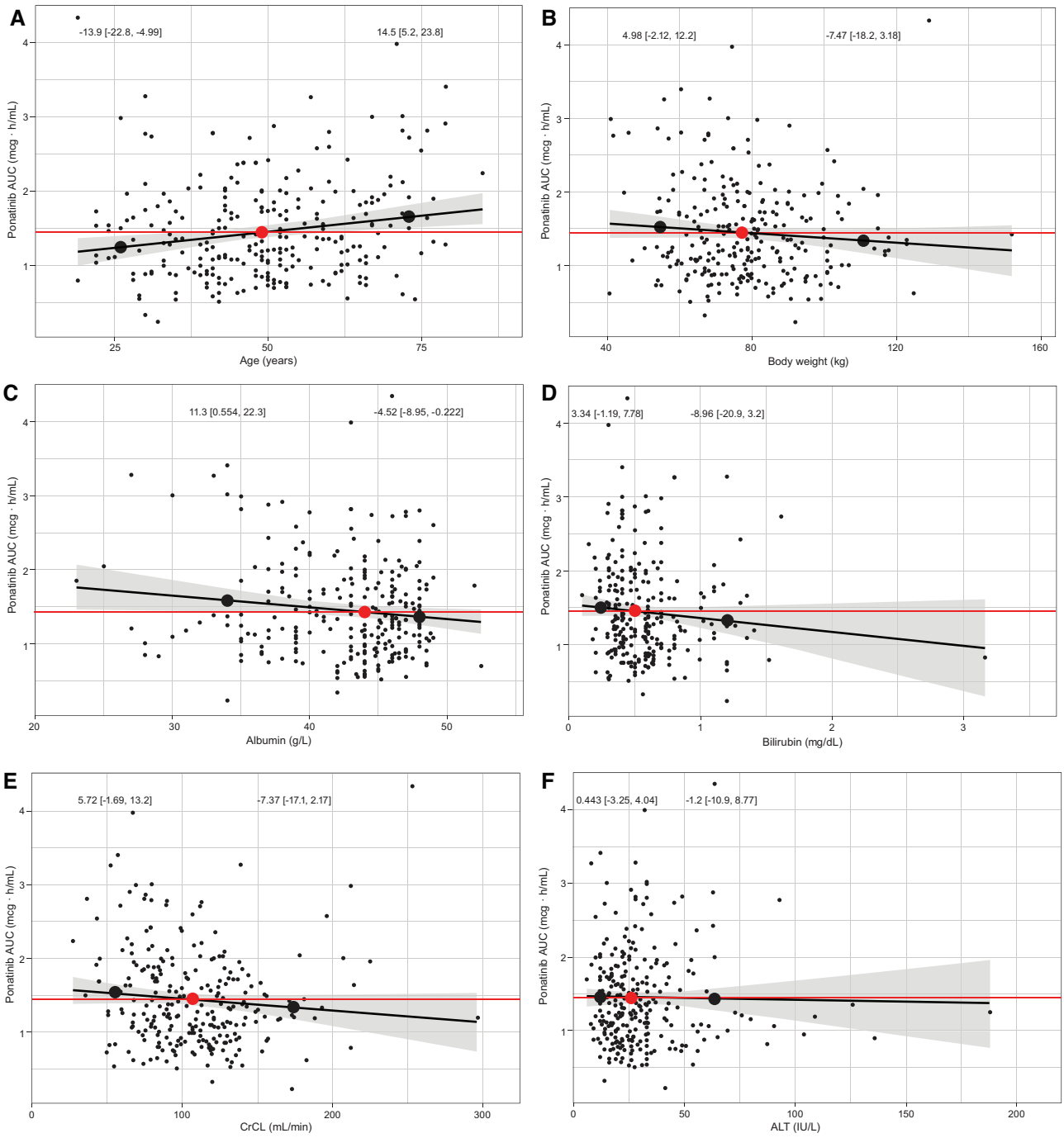

Figure 3. (A-F). Individual predicted ponatinib steady-state exposures (45 mg once daily) vs continuous covariates: age (A), body weight (B), serum albumin (C), bilirubin (D), CrCL (E), and ALT (F). Small black circles represent individual ponatinib exposures; black line (gray-shaded area) represents a linear regression (95%CI) of individual exposures vs covariate; numbers [ranges] at the top of the plots are changes in percent [95%CI] in ponatinib exposure predicted by the linear regression at the 5th or 95th percentile of individual covariate values (large black circles) relative to the predicted AUC at the median of individual covariate values (red circle and horizontal line). (G-I) Individual predicted exposures vs categorical covariates: sex (G), disease status (H), and race (I). Boxplots represent distributions of individual ponatinib exposures vs covariates; numbers [ranges] at the top of the plots are changes in percent [95%CI] in ponatinib mean exposure at categorical covariate values (large black circles) relative to the predicted AUC in the most common covariate category (red circle and horizontal line); numbers below each box represent the sample size within each category. ALT, alanine aminotransferase; AUC, area under the plasma concentration–time curve; CI, confidence interval; CrCL, creatinine clearance; HV, healthy volunteers; Pts, patients.

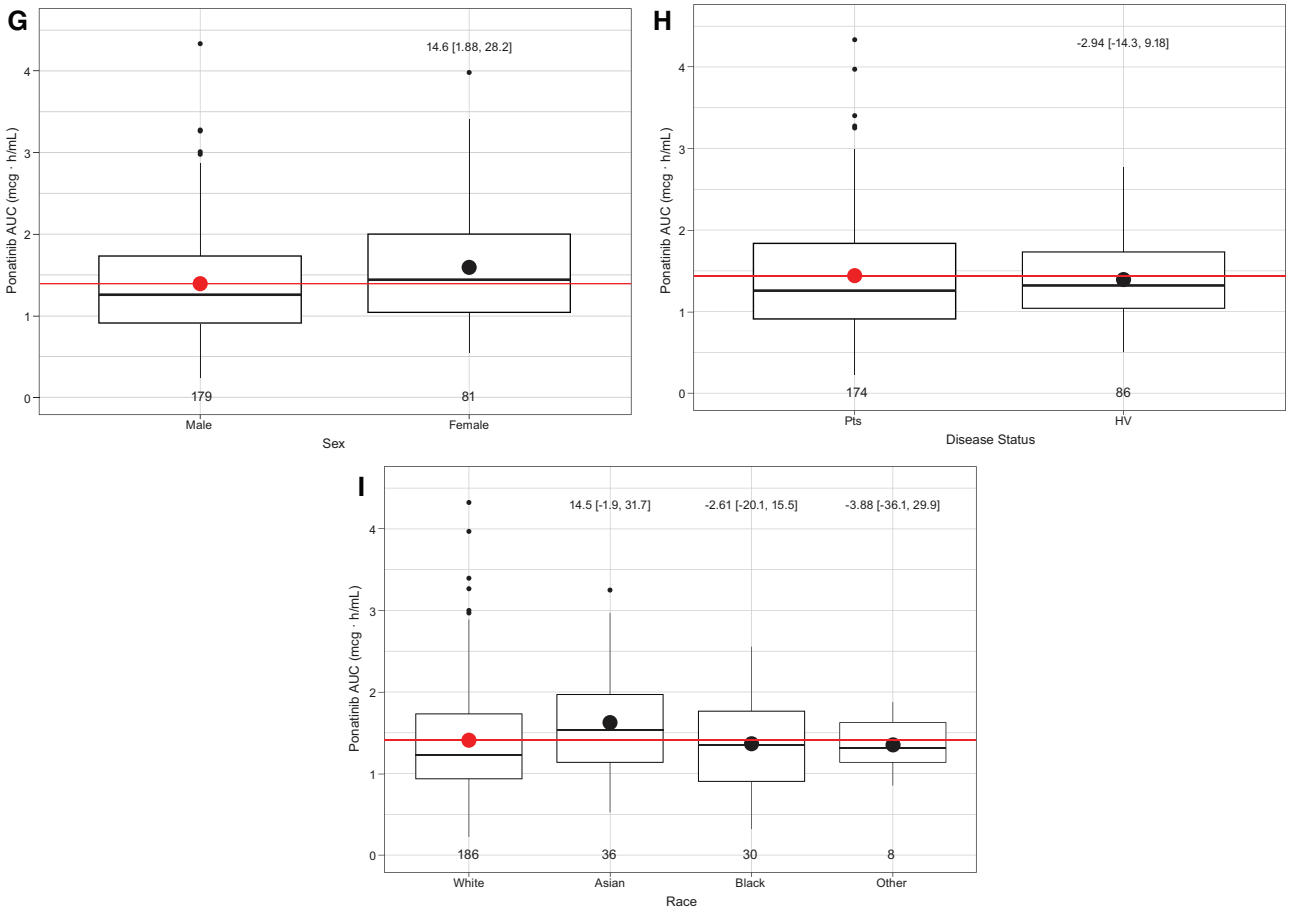

Figure 3. *Continued*

Discussion

This population PK analysis of the oral TKI ponatinib provides a comprehensive model-based integration of data from 260 participants (174 patients and 86 healthy volunteers) enrolled across 7 clinical trials, including 5 phase 1 studies,[8–11,13] 1 phase 1/2 study,[12] and 1 phase 3 study.[14] The PK of ponatinib was adequately described by a 2-compartment model with linear first-order elimination from the central compartment. The absorption component of the model consisted of 2 routes of absorption where the first route of absorption was described by 2 discrete transit compartments, and the second route was described by a delayed first-order absorption process. While the absorption in patients could be described solely by the first absorption route, absorption in healthy volunteers necessitated a split of the absorbed dose between the 2 routes. The need for the complex absorption profile in the healthy volunteer group appeared to be driven in part by differences in the study designs and PK sampling schemes employed across the clinical program. Data obtained from the studies in patients with hematologic malignancies[12–14] was based on a heterogeneous mix of patients with varying degrees of comorbidities and concomitant medications, and PK samples were obtained predominantly following repeated doses. In contrast, PK samples in the healthy volunteer trials were obtained following single doses of ponatinib under a strict serial sampling schedule. The final population PK model included individual random effects on CL/F, V3/F, and K_{a1}. The correlation between random effects for CL/F and V3/F was estimated in the model to improve fit and allow the model to reproduce the observed correlation in simulations.

Multivariate stepwise covariate modeling did not identify significant effects of any covariates on CL/F. Age and body weight were the only covariates that had statistically significant effects on V3/F. The effects of these covariates on V3/F did not influence overall systemic exposure (AUC), were small relative to the overall variability of ponatinib V3/F in the patient population, and were therefore not considered to be of clinical significance. To further confirm the selected covariate model and the lack of an impact on total systemic exposure of ponatinib (AUC), relationships between individual model-predicted ponatinib AUC and covariates were explored. For continuous and categorical

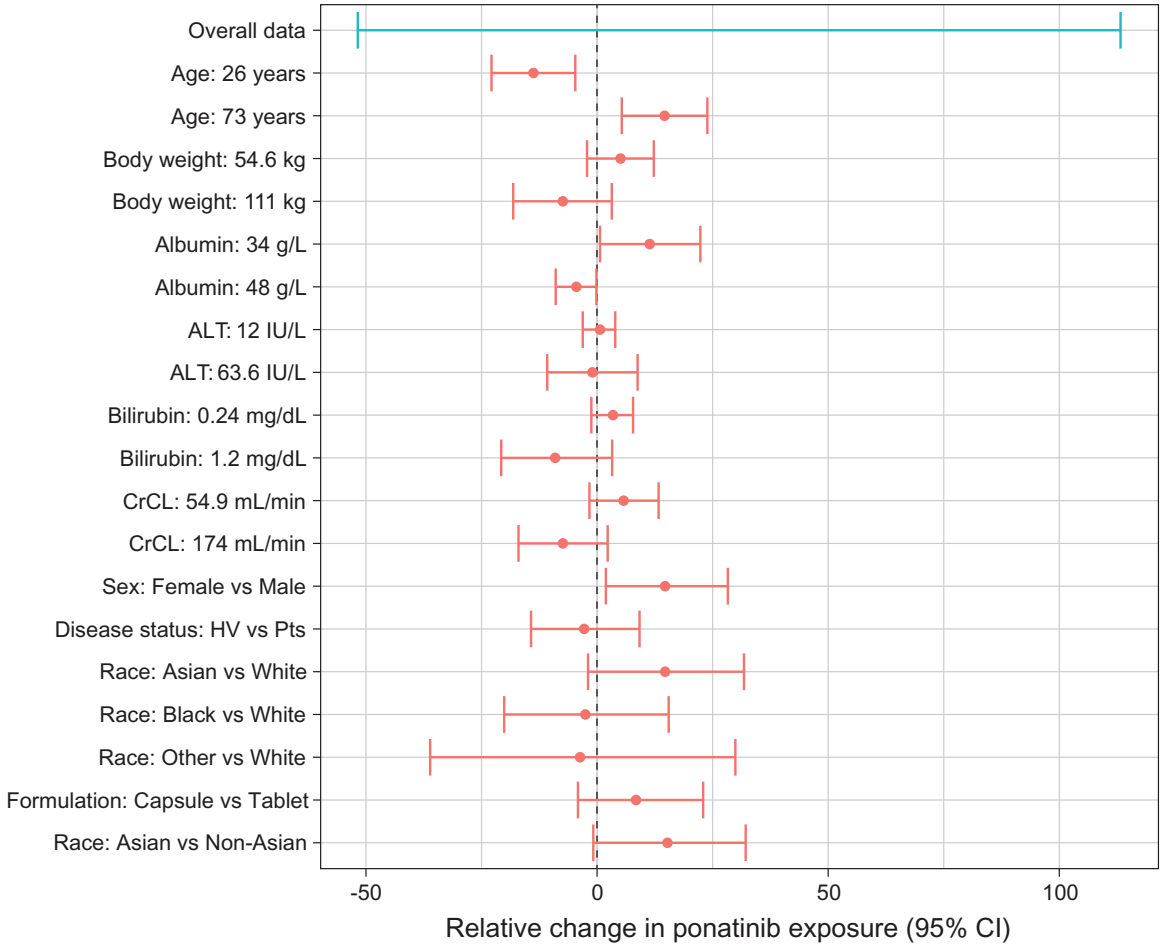

Figure 4. Magnitude of covariate effects relative to the overall population on individual predicted estimates of ponatinib exposure. The horizontal blue bar shows the 5th to 95th percentile range of ponatinib exposures relative to the median of individual predicted exposures. Red circles (error bars) show exposures (95%CI) at the 5th and 95th percentile of a covariate compared with exposure at the median (continuous covariates) or exposures for a covariate category relative to the reference (most common) category. ALT, alanine aminotransferase; CI, confidence interval; CrCL, creatinine clearance; HV, healthy volunteers; Pts, patients.

covariates, the model-predicted exposure at the 5th and 95th percentiles of the covariate fell within –13.9% and 15.1% of the exposure at the median covariate value, respectively. Based on these findings, it was concluded that patient-specific factors, including albumin (23-52.5 g/L), sex, age (19-85 years), body weight (40.7-152 kg), total bilirubin (0.1-3.16 mg/dL), ALT (6-188 U/L), creatinine clearance (27.8-296 mL/min), and race (including Asian race), did not contribute to clinically important differences in ponatinib exposure. Of note, a common global dose without adjustment for any baseline covariates was used during the clinical development of ponatinib. The lack of an effect of mild and moderate renal impairment (ie, creatinine clearance ≥30 mL/min) is consistent with metabolism being the primary route of clearance for ponatinib as there was negligible urinary excretion of ponatinib in the radiolabeled mass balance study.[7]

The final model was then used to simulate ponatinib plasma concentrations at varying doses in a patient population. In cell-based assays, a ponatinib concentration of 20 nM (10.7 ng/mL) was sufficient to suppress most *BCR-ABL1* mutant clones and a concentration of 40 nM (21.3 ng/mL) completely suppressed T315I mutant clones.[1] In the simulations using the final population PK model, ponatinib doses of 15 to 45 mg once daily were predicted to result in steady-state $C_{average}$ values that approximated or exceeded these concentrations associated with in vitro pharmacological activity of ponatinib. The comparison of total plasma concentrations to in vitro potency estimates without corrections for plasma protein binding is supported by data demonstrating that the presence of physiologically relevant concentrations of albumin had no meaningful impact on the cellular potency of ponatinib.[22]

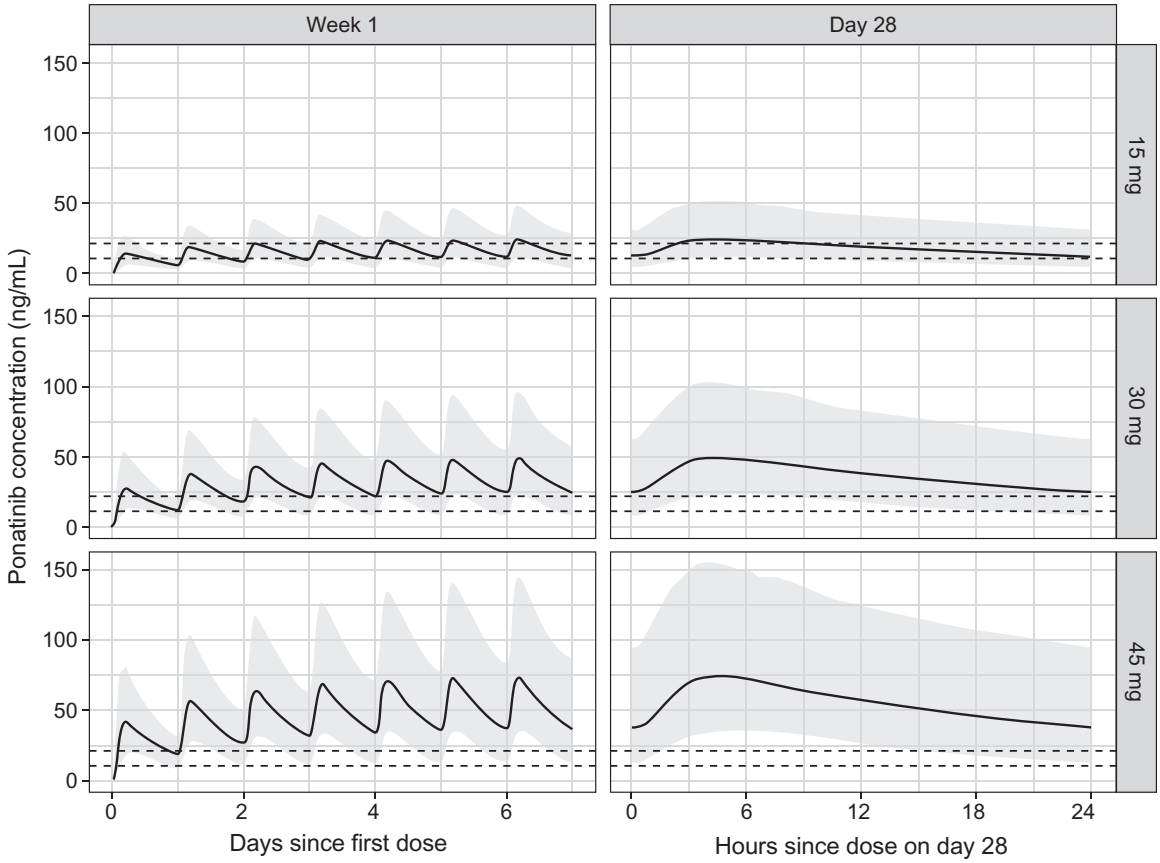

Figure 5. Simulated ponatinib concentrations vs time in the first week (left panels) and over the day 28 dosing interval (right panels) of once-daily dosing with 15 mg, 30 mg, or 45 mg. Solid black lines show the ponatinib plasma concentration–time profile predicted for the typical patient; shaded areas show the 5th to 95th percentiles of concentration-time profiles predicted for 1000 virtual patients; horizontal dashed lines represent concentrations of ponatinib associated with inhibition of *BCR-ABL1* (10.7 ng/mL) and T315I mutants (21.3 ng/mL) in cell-based assays.

Ponatinib was initially approved in 2012. However, subsequent to its approval, a dose-optimization study (NCT02467270; OPTIC) was initiated due to long-term safety data indicating a risk for arterial occlusive events. The OPTIC (Optimizing Ponatinib Treatment in Chronic Myeloid Leukemia) study was designed to evaluate starting doses of ponatinib 45 mg, 30 mg, and 15 mg once daily with a mandatory dose reduction to 15 mg once daily upon achievement of $\leq$1% *BCR-ABL1*/*ABL1*^{IS} for patients receiving 45 mg or 30 mg of ponatinib.[23] The results of the current population PK analysis indicate that exposures achieved with doses of 15 to 45 mg are within the pharmacologically active range for *BCR-ABL1* inhibition, thereby supporting the selection of these doses for evaluation of dose-response for efficacy and safety in OPTIC.

Because no pediatric clinical PK data are currently available for ponatinib, an allometric scaling approach was used to project pediatric PK using the developed adult population PK model. The use of allometry was supported by knowledge of clearance mechanisms for ponatinib and their corresponding ontogeny. Specifically, ponatinib is metabolized predominantly by CYP3A with additional contributions by esterases and/or amidases. These clearance mechanisms are expected to approach adult levels within the first year of life.[24–27] The results of these simulations using the allometrically adapted model supported the selection of weight-binned posology for pediatric development (ClinicalTrials.gov Identifier: NCT04501614).

Conclusions

Ponatinib PK was described by a 2-compartment model with linear first-order elimination. Covariates of interest, including sex, age, race, body weight, total bilirubin, ALT, albumin, and CrCL did not have clinically meaningful effects on the PK of ponatinib, suggesting that no dose adjustment is required based on these covariates. Doses of 15 to 45 mg resulted in exposures within the pharmacologically active range for *BCR-ABL1* inhibition. Simulations from the final model were used to inform dose selection for pediatric development.

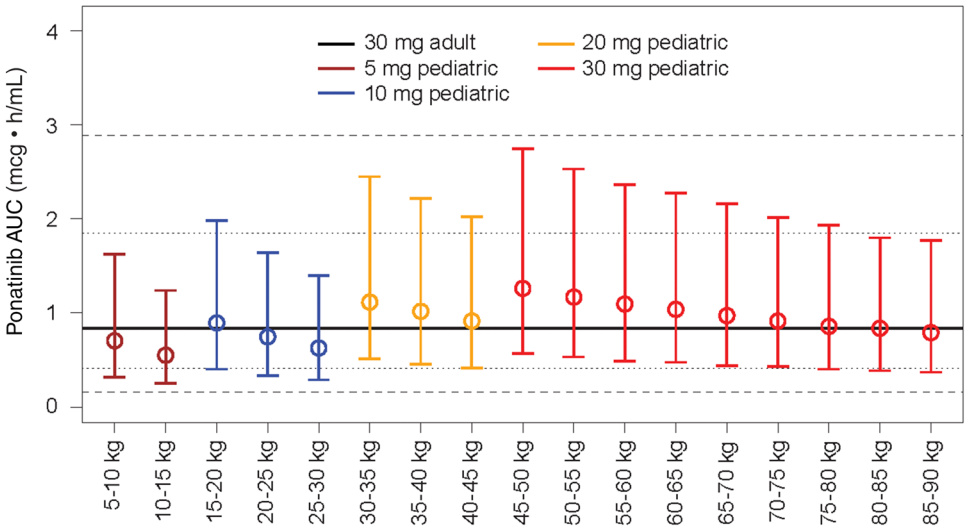

Figure 6. Predicted pediatric exposures of ponatinib in patients receiving 30 mg (body weight ≥45 kg), 20 mg (≥30 and <45 kg), 10 mg (≥15 and <30 kg), or 5 mg (≥5 and <15 kg) compared with adult exposures at 30 mg. Circles (error bars) denote the median (5th to 95th percentile) of AUC for pediatric patients in each 5-kg body weight bin. The solid black line represents the median of AUC for adult patients as estimated from the population PK analysis; dotted lines represent the 5th and 95th percentiles and dashed lines represent the range for adult patients. AUC, area under the plasma concentration–time curve; PK, pharmacokinetic.

Acknowledgments

The authors would like to thank the patients, their families, and their caregivers; the study investigators and their team members at each study site; and colleagues from Millennium Pharmaceuticals, Inc., Cambridge, Massachusetts, a wholly owned subsidiary of Takeda Pharmaceutical Company Limited. Professional medical writing assistance was provided by Lauren Gallagher, RPh, PhD, and Lela Creutz, PhD, of Peloton Advantage, LLC, an OPEN Health company, Parsippany, New Jersey, and funded by Millennium Pharmaceuticals, Inc., Cambridge, Massachusetts, a wholly owned subsidiary of Takeda Pharmaceutical Company Limited.

Conflicts of Interest

M.H. is an employee of Takeda Pharmaceutical Company Limited. P.D. is an employee of Certara and consultant to Takeda Pharmaceutical Company Limited. N.N. is a previous employee of ARIAD Pharmaceuticals, a wholly owned subsidiary of Takeda Pharmaceutical Company Limited. S.S. is a previous employee of Takeda Pharmaceutical Company Limited. N.G. is an employee of Takeda Pharmaceutical Company Limited. K.V. is a previous employee of Takeda Pharmaceutical Company Limited.

Data Availability Statement

The data sets, including the redacted study protocol, redacted statistical analysis plan, and individual participant data supporting the results reported in this article, will be made available within 3 months from initial request, to researchers who provide a methodologically sound proposal. The data will be provided after deidentification, in compliance with applicable privacy laws, data protection, and requirements for consent and anonymization.

References

1. O'Hare T, Shakespeare WC, Zhu X, et al. AP24534, a pan-BCR-ABL inhibitor for chronic myeloid leukemia, potently inhibits the T315I mutant and overcomes mutation-based resistance. *Cancer Cell*. 2009;16(5):401-412.
2. Deininger MW, Hodgson JG, Shah NP, et al. Compound mutations in BCR-ABL1 are not major drivers of primary or secondary resistance to ponatinib in CP-CML patients. *Blood*. 2016;127(6):703-712.
3. Baccarani M, Deininger MW, Rosti G, et al. European LeukemiaNet recommendations for the management of chronic myeloid leukemia: 2013. *Blood*. 2013;122(6):872-884.
4. *Iclusig [package insert]*. Cambridge, MA: Takeda Pharmaceutical Company Limited; 2020.
5. Cortes JE, Kim DW, Pinilla-Ibarz J, et al. A phase 2 trial of ponatinib in Philadelphia chromosome-positive leukemias. *N Engl J Med*. 2013;369(19):1783-1796.
6. Cortes JE, Kim DW, Pinilla-Ibarz J, et al. Ponatinib efficacy and safety in Philadelphia chromosome−positive leukemia: final 5-year results of the phase 2 PACE trial. *Blood*. 2018;132(4):393-404.
7. Ye YE, Woodward CN, Narasimhan NI. Absorption, metabolism, and excretion of [(14)C] ponatinib after a single oral dose in humans. *Cancer Chemother Pharmacol*. 2017;79(3):507-518.
8. Narasimhan NI, Dorer DJ, Niland K, Haluska F, Sonnichsen D. Effects of food on the pharmacokinetics of ponatinib in healthy subjects. *J Clin Pharm Ther*. 2013;38(6):440-444.
9. Narasimhan NI, Dorer DJ, Niland K, Haluska F, Sonnichsen D. Effects of ketoconazole on the pharmacokinetics of ponatinib in healthy subjects. *J Clin Pharmacol*. 2013;53(9):974-981.
10. Narasimhan NI, Dorer DJ, Davis J, Turner CD, Sonnichsen D. Evaluation of the effect of multiple doses of lansoprazole on the

pharmacokinetics and safety of ponatinib in healthy subjects. *Clin Drug Investig*. 2014;34(10):723-729.
11. Narasimhan NI, Dorer DJ, Davis J, Turner CD, Sonnichsen D. Evaluation of the effect of multiple doses of rifampin on the pharmacokinetics and safety of ponatinib in healthy subjects. *Clin Pharmacol Drug Develop*. 2015;4(5):354-360.
12. Tojo A, Kyo T, Yamamoto K, et al. Ponatinib in Japanese patients with Philadelphia chromosome-positive leukemia, a phase 1/2 study. *Int J Hematol*. 2017;106(3):385-397.
13. Cortes JE, Kantarjian H, Shah NP, et al. Ponatinib in refractory Philadelphia chromosome-positive leukemias. *N Engl J Med*. 2012;367(22):2075-2088.
14. Lipton JH, Chuah C, Guerci-Bresler A, et al. Ponatinib versus imatinib for newly diagnosed chronic myeloid leukaemia: an international, randomised, open-label, phase 3 trial. *Lancet Oncol*. 2016;17(5):612-621.
15. Bauer RJ. *NONMEM Users Guide: Introduction to NONMEM 7.3.0*. Gaithersburg, MD: ICON Development Solutions; 2015.
16. R Development Core Team. *R: A Language and Environment for Statistical Computing*. Vienna, Austria; 2013.
17. Savic RM, Karlsson MO. Importance of shrinkage in empirical Bayes estimates for diagnostics: problems and solutions. *AAPS J*. 2009;11(3):558-569.
18. Wahlby U, Jonsson EN, Karlsson MO. Comparison of stepwise covariate model building strategies in population pharmacokinetic-pharmacodynamic analysis. *AAPS Pharm Sci*. 2002;4(4):E27.
19. Centers for Disease Control and Prevention, National Center for Health Statistics. Selected percentiles and LMS parameters. www.cdc.gov/growthcharts/percentile_data_files.htm. Accessed November 3, 2021.
20. *Gleevec [package insert]*. East Hanover, NJ: Novartis Pharmaceuticals Corporation; 2020.
21. Savic RM, Jonker DM, Kerbusch T, Karlsson MO. Implementation of a transit compartment model for describing drug absorption in pharmacokinetic studies. *J Pharmacokinet Pharmacodyn*. 2007;34(5):711-726.
22. Huang WS, Metcalf CA, Sundaramoorthi R, et al. Discovery of 3-[2-(imidazo[1,2-b]pyridazin-3-yl)ethynyl]-4-methyl-N-{4-[(4-methylpiperazin-1-yl)-methyl]-3-(trifluoromethyl)phenyl} benzamide (AP24534), a potent, orally active pan-inhibitor of breakpoint cluster region-abelson (BCR-ABL) kinase including the T315I gatekeeper mutant. *J Med Chem*. 2010;53(12):4701-4719.
23. Cortes JE, Lomaia E, Turkina A, et al. Interim analysis (IA) of OPTIC: A dose-ranging study of three ponatinib (PON) starting doses [abstract]. *J Clin Oncol*. 2020;38(15 suppl):7502.
24. de Wildt SN, Kearns GL, Leeder JS, van den Anker JN. Cytochrome P450 3A: ontogeny and drug disposition. *Clin Pharmacokinet*. 1999;37(6):485-505.
25. Boberg M, Vrana M, Mehrotra A, et al. Age-dependent absolute abundance of hepatic carboxylesterases (CES1 and CES2) by LC-MS/MS proteomics: application to PBPK modeling of oseltamivir in vivo pharmacokinetics in infants. *Drug Metab Dispos*. 2017;45(2):216-223.
26. Upreti VV, Wahlstrom JL. Meta-analysis of hepatic cytochrome P450 ontogeny to underwrite the prediction of pediatric pharmacokinetics using physiologically based pharmacokinetic modeling. *J Clin Pharmacol*. 2016;56(3):266-283.
27. Salem F, Johnson TN, Abduljalil K, Tucker GT, Rostami-Hodjegan A. A re-evaluation and validation of ontogeny functions for cytochrome P450 1A2 and 3A4 based on in vivo data. *Clin Pharmacokinet*. 2014;53(7):625-636.

Supplemental Information

Additional supplemental information can be found by clicking the Supplements link in the PDF toolbar or the Supplemental Information section at the end of web-based version of this article.